Increased efficiency in multijunction solar cells through the incorporation of semimetallic ErAs nanoparticles into the tunnel junction

J. M. O. Zide,[a] A. Kleiman-Shwarsctein, N. C. Strandwitz, J. D. Zimmerman, T. Steenblock-Smith, and A. C. Gossard
Materials Department, University of California, Santa Barbara, California 93106

A. Forman, A. Ivanovskaya, and G. D. Stucky
Chemistry Department, University of California, Santa Barbara, California 93106

(Received 17 November 2005; accepted 12 March 2006; published online 17 April 2006)

We report the molecular beam epitaxy growth of $Al_{0.3}Ga_{0.7}As/GaAs$ multijunction solar cells with epitaxial, semimetallic ErAs nanoparticles at the interface of the tunnel junction. The states provided by these nanoparticles reduce the bias required to pass current through the tunnel junction by three orders of magnitude, and therefore drastically reduce the voltage losses in the tunnel junction. We have measured open-circuit voltages which are 97% of the sum of the constituent cells, which result in nearly double the efficiency of our multijunction cell with a conventional tunnel junction. © *2006 American Institute of Physics*. [DOI: 10.1063/1.2196059]

Currently, multijunction solar cells have the highest solar cell energy conversion efficiencies. However, the tunnel junction interconnects generally used within multijunction solar cells result in losses which limit the performance of the device. Multijunction solar cells for terrestrial applications are typically used under concentrated (many sun) conditions. Here, an enhanced tunnel junction with a low resistance and a large peak current density would be quite beneficial. Furthermore, the current density of a multijunction solar cell containing a wider-band-gap tunnel junction can, in principle, be larger due to decreased absorption of photons within the tunnel junction. However, the performance of conventional tunnel junctions suffers in wider-band-gap materials, such as AlGaAs or GaInP, where tunneling current is reduced substantially for a particular bias.[1] An enhanced tunnel junction technology could allow high-performance wider-band-gap tunnel junctions and resulting increases in device performance. Such an improved tunnel junction technology may also facilitate the growth of many-junction cells in which the tunnel junction stability during growth is a concern. In this letter, we describe the use of semimetallic nanoparticles to create improved tunnel junctions in multijunction solar cells.

Incorporating semimetallic nanoparticles into a semiconductor drastically changes the various properties of the semiconductor. More specifically, ErAs is a rocksalt semimetal which grows epitaxially via the Volmer-Weber (island) growth mode on GaAs.[2] For sufficiently small depositions, nanoparticles are formed which can be overgrown by GaAs without introducing defects. The particles can act as dopants,[3] buried Schottky barriers,[4] or phonon scattering centers.[5,6] They can enhance thermoelectric materials[7] or provide deep states for rapid carrier recombination.[2] These deep states can also enhance the performance of tunnel junctions.[8] The presence of midgap states at the p^+-n^+ interface allows tunneling to occur via a two-step process, and therefore it effectively halves the tunneling distance for each step (Fig. 1). Because tunneling probability decreases exponentially with both barrier height and distance, this two-step tunneling process results in a drastic reduction in the bias required to pass a particular current. Room temperature *J-V* curves comparing a conventional GaAs tunnel junction to a similar tunnel junction with small islands of ErAs at the interface are shown in Fig. 2. We demonstrate the use of these ErAs-enhanced tunnel junctions in multijunction solar cells.

Multijunction solar cells consist of two or more vertically stacked, interconnected solar cells, each of which consists of a semiconductor *p-n* junction. The band gap of the semiconductor which comprises each cell decreases with depth into the structure. This allows multijunction cells to achieve higher efficiencies than single-junction cells by collecting higher-energy photons at a larger voltage in the wider-band-gap top cell while still collecting lower-energy photons (which are not absorbed in the top cell) in the narrower-band-gap bottom cell. Two-junction cells consisting of $Ga_{0.5}In_{0.5}P$ top cells and GaAs bottom cells[9–12] have achieved efficiencies as high as 30.28%.[10,11] The use of $Al_xGa_{1-x}As$ as a top cell has been studied,[13–15] but it is not typically used since AlGaAs has relatively short minority carrier diffusion lengths (compared with the absorption length for photons) due to nonradiative recombination caused by high concentrations of defects. This results in decreased photocurrent and therefore limits overall device performance.

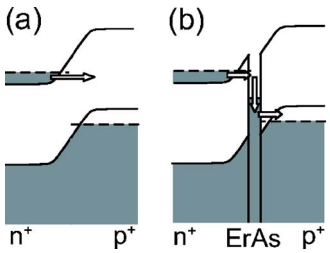

FIG. 1. Schematic band diagram of tunnel junctions under forward bias. (a) Conventional tunnel junction; the lack of equal-energy states in the p^+ side results in a small tunneling current. (b) ErAs-enhanced tunnel junction; the presence of midgap states allows tunneling to occur via a two-step process, resulting in a much larger tunneling current.

[a]Electronic mail: jmz@engineering.ucsb.edu

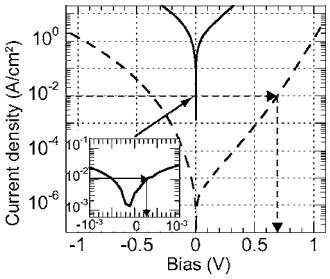

FIG. 2. Room temperature *J-V* curves for conventional tunnel junctions (dashed curve) and ErAs-enhanced tunnel junctions (solid curve and inset). For a current density of 10 mA/cm^2 (a typical value for a multijunction solar cell), ~0.7 V of bias is required for the conventional tunnel junction while ~0.3 mV is required for the ErAs-enhanced tunnel junction.

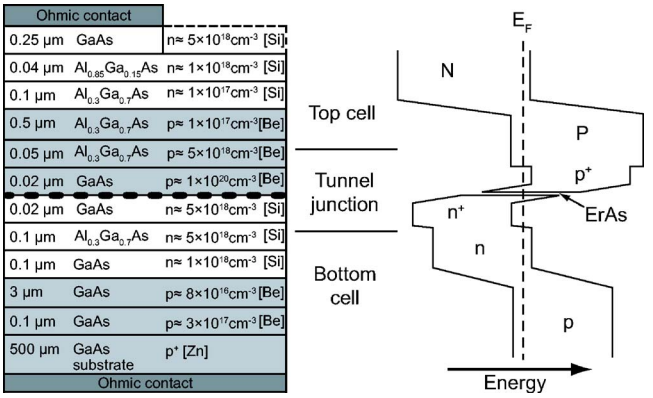

FIG. 3. Growth structure and schematic band diagram of AlGaAs/GaAs multijunction cell. The dots in the middle of the tunnel junction represent 1.2 monolayers of ErAs, which form nanoparticles with ~30% layer coverage.

Most multijunction solar cells are two-terminal monolithic devices with degenerately doped p^+-n^+ tunnel junctions used as interconnects. These tunnel junctions consist of an interface between heavily doped n^+ and p^+ layers; the heavy doping results in a short depletion width, creating a thin barrier for tunneling. Electrons in the conduction band of the n^+ layer can tunnel into states in the valence band of the p^+ layer. Each of the constituent solar cells consists of a semiconductor *p-n* junction in which absorbed photons produce carriers which are separated across the depletion region, resulting in a photovoltage across the diode. The photovoltage of a multijunction cell is the sum of the photovoltages of the individual cells less voltage drops in the interconnect and contacts. Because the multijunction cell is a series device, the short-circuit photocurrent I_{SC} (and the short-circuit current density J_{SC}) is limited by the smallest photocurrent produced in any of the constituent cells. The maximum power and efficiency occur at the resistive load for which *VI* is maximized; the voltage and current density at this load are given by V_M and J_M, respectively. Maximum efficiency is achieved when the cells are current matched (which is generally achieved by carefully selecting the thickness and/or band gaps of each cell) and the voltage losses in the interconnect are minimized. Therefore, tunnel junctions with minimal voltage losses are essential for efficient multijunction solar cells. While extensive work has gone into designing and optimizing growth parameters for tunnel junctions in solar cell applications,[10–12,15,16] the voltage losses remain a concern.

There are several sources of these voltage losses in conventional tunnel junctions. Because the current density J_M must pass through the tunnel junction, the tunnel junction must be forward biased to allow recombination of that current density. Given that J_M in a typical multijunction solar cell is on the order of 10 mA/cm^2, Fig. 2 indicates that a bias of ~0.7 V is required for our conventional tunnel junction. While a state-of-the-art conventional tunnel junction would have a smaller resistance, the V_M for a multijunction solar cell containing this particular tunnel junction is reduced by ~0.7 V. In comparison, the bias required for the same current density in an ErAs-enhanced tunnel junction (which is otherwise identical to this nonoptimized conventional tunnel junction) is only ~0.3 mV.

An additional voltage loss occurs due to photons absorbed within the tunnel junction and in the immediate vicinity. Carriers excited by the incident photons absorbed within the tunnel junction create a recombination current (and therefore a bias to compensate) across the tunnel junction. It is also expected that carriers photoexcited in an undepleted region of the top cell within the minority carrier diffusion length of the tunnel junction interface would diffuse and recombine across the tunnel junction, producing additional bias. The photovoltage produced by these absorbed photons will have opposite polarity from that in the top and bottom cells and will therefore decrease the voltage of the multijunction solar cell. The decrease in V_{OC} is expected to be comparable in magnitude to the reduction in V_M described above.

To test the effects of ErAs-enhanced tunnel junctions within multijunction solar cells experimentally, we prepared $Al_{0.3}Ga_{0.7}As$/GaAs multijunction solar cells with both conventional tunnel junctions and ErAs-enhanced tunnel junctions. $Al_{0.3}Ga_{0.7}As$ was used for the top cell because the goal of this work was to elucidate the effects of an enhanced tunnel junction rather than to achieve an especially high efficiency. We have also prepared $Al_{0.3}Ga_{0.7}As$ and GaAs single-junction solar cells. All samples were grown using a Varian Gen II molecular beam epitaxy (MBE) system on (100) *p*-type (Zn-doped) GaAs substrates. Silicon and beryllium were used as *n*-type and *p*-type dopants, respectively. The structure of the multijunction cell with the ErAs-enhanced tunnel junction and a schematic representation of the band structure are shown in Fig. 3. The structure of the other samples is based closely on this structure; the single-junction cells are identical to the constituent cells within the multijunction cells. In the case of the ErAs-enhanced tunnel junctions, 1.2 monolayers (MLs) of ErAs were deposited, which correspond to approximately 30% surface coverage of nanoparticles which are approximately 4 MLs in height. Details of the ErAs growth have been discussed previously.[2]

Using the MBE-grown structure, solar cells with an area of 0.25 cm^2 were fabricated using standard photolithographic techniques. Ohmic contacts in the form of a contact pad and metal wires were evaporated on the top using Pd/Ge/Ti/Pt/Au. The top contact eclipsed approximately 5% of the incident light. The back side Ohmic contact was formed using evaporated Pd/Ti/Pd/Au on the entire back side of the device. Devices were annealed in forming gas for 1 min at 450 °C. The remainder of the *n*-GaAs contact layer was removed after metallization using citric acid: H_2O_2. No antireflective coating was used.

These solar cells were illuminated using the filtered output of a Xe lamp. A portion of the far-infrared spectrum was

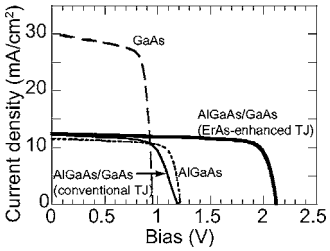

FIG. 4. *J-V* curves of single-junction and multijunction solar cells. The dashed curve represents a GaAs cell, while the dotted curve is an $Al_{0.3}Ga_{0.7}As$ cell. The light solid curve is a two-junction AlGaAs/GaAs cell with a conventional tunnel junction while the heavier solid curve is a two-junction AlGaAs/GaAs cell with an ErAs-enhanced tunnel junction.

attenuated using a water filter and a 400 nm cutoff filter was used to approximate the air-mass 1.5 (AM1.5) spectrum (one sun conditions). All measurements were performed under 100 mW/cm^2 illumination as measured with a radiometer. The *J-V* characteristics of several solar cells fabricated from each sample were measured using a Keithley source meter. A representative *J-V* curve for each type of device is shown in Fig. 4. The average values of open-circuit voltage, short-circuit current density, fill factor $[FF=V_M J_M/(V_{OC}J_{SC})]$, and efficiency for each cell are given in Table I.

As is typical of AlGaAs/GaAs multijunction solar cells,[14,15] current-matched conditions were not achieved. The current density of both multijunction cells was limited to that of the AlGaAs cell. The open-circuit voltage of the multijunction cell with the ErAs-enhanced tunnel junction was 97% of the sum of the open-circuit voltages of the AlGaAs and GaAs cells. This sum would be the open-circuit voltage for a multijunction solar cell with a lossless tunnel junction. In contrast, the open-circuit voltage of the multijunction cell with a conventional tunnel junction is reduced by nearly 1 V to 53% of the sum of the open-circuit voltages of the GaAs and AlGaAs cells. This reduced voltage is likely due to rectification in the conventional tunnel junction as described above; the photovoltage produced in the tunnel junction has opposite polarity of that produced in the top and bottom cells. Because of this voltage difference, the efficiency of the multijunction cell with the ErAs-enhanced tunnel junction is approximately double the efficiency of the multijunction cell with a conventional tunnel junction. In all cases, the fill factor is reasonably large, indicating high quality solar cells.

TABLE I. Measured characteristics of single- and multijunction solar cells. All quantities are averages of measurements on several devices. Cell size was 0.25 cm^2.

Structure	V_{OC} (V)	J_{SC} (mA/cm^2)	FF	Eff. (%)
GaAs	0.97	30.4	0.71	22.7
AlGaAs	1.18	11.4	0.68	10.3
AlGaAs/GaAs conventional TJ	1.14	12.0	0.77	9.3
AlGaAs/GaAs ErAs-enhanced TJ	2.08	12.2	0.77	18.1

The efficiency of each multijunction cell is lower than that of the isolated GaAs cell, which illustrates the performance limitations of these device designs. The main limitation is the use of AlGaAs for the wider-band-gap cell; it is difficult to generate large photocurrent densities in an AlGaAs cell due to defects which allow exciton recombination.[13] The poor performance of the conventional tunnel junction demonstrates the difficulty of making high quality tunnel junctions using conventional designs. The performance enhancement of these tunnel junctions illustrates the importance of incorporating metal nanoparticles into tunnel junctions; the technique allows high-performance tunnel junctions where they would otherwise be difficult or impossible to realize. Additionally, this technique could be applied to wider-band-gap tunnel junctions, where a two-step tunneling process reduces the bias required for a given tunneling current. Also, it is worth considering the wider applicability of incorporating metal nanoparticles to creating high-performance tunnel junctions using other growth methods which might result in lower-cost multijunction solar cells.

The authors would like to thank Gottfried Döhler, Eric W. McFarland, Brian Thibeault, and Martin Vandenbroek for helpful discussions of physics and processing. The authors would also like to acknowledge the support of the NSF nanofabrication facilities at the University of California, Santa Barbara. This work was partially funded by an ONR grant monitored by Dr. Colin Wood and by a gift from Corning.

[1] S. M. Sze, *Physics of Semiconductor Devices*, 2nd ed. (Wiley, New York, 1981).
[2] C. Kadow, S. B. Fleischer, J. P. Ibbetson, J. E. Bowers, and A. C. Gossard, Appl. Phys. Lett. **75**, 3548 (1999).
[3] D. C. Driscoll, M. Hanson, C. Kadow, and A. C. Gossard, Appl. Phys. Lett. **78**, 1703 (2001).
[4] A. Dorn, M. Peter, S. Kicin, T. Ihn, K. Ensslin, D. Driscoll, and A. C. Gossard, Appl. Phys. Lett. **82**, 2631 (2003).
[5] D. G. Cahill, K. Goodson, and A. Majumdar, J. Heat Transfer **124**, 223 (2002).
[6] D. G. Cahill, W. K. Ford, K. E. Goodson, G. D. Mahan, A. Majumdar, H. J. Maris, R. Merlin, and S. R. Phillpot, J. Appl. Phys. **93**, 793 (2003).
[7] J. M. Zide, D. O. Klenov, S. Stemmer, A. C. Gossard, G. Zeng, J. E. Bowers, D. Vashaee, and A. Shakouri, Appl. Phys. Lett. **87**, 112102 (2005).
[8] P. Pohl, F. H. Renner, M. Eckardt, A. Schwanhausser, A. Friedrich, O. Yuksekdag, S. Malzer, G. H. Dohler, P. Kiesel, D. Driscoll, M. Hanson, and A. C. Gossard, Appl. Phys. Lett. **83**, 4035 (2003).
[9] J. M. Olson, S. R. Kurtz, A. E. Kibbler, and P. Faine, Appl. Phys. Lett. **56**, 623 (1990).
[10] T. Takamoto, E. Ikeda, H. Kurita, and M. Ohmori, Appl. Phys. Lett. **70**, 381 (1997).
[11] T. Takamoto, E. Ikeda, H. Kurita, M. Ohmori, M. Yamaguchi, and Yang Ming-Ju, Jpn. J. Appl. Phys., Part 1 **36**, 6215 (1997).
[12] M. Y. Feteha and G. M. Eldallal, Renewable Energy **28**, 1097 (2003).
[13] C. Amano, H. Sugiura, K. Ando, M. Yamaguchi, and A. Saletes, Appl. Phys. Lett. **51**, 1075 (1987).
[14] C. Amano, H. Sugiura, A. Yamamoto, and M. Yamaguchi, Appl. Phys. Lett. **51**, 1998 (1987).
[15] C. Amano, H. Sugiura, M. Yamaguchi, and K. Hane, IEEE Trans. Electron Devices **36**, 1026 (1989).
[16] M. Yamaguchi, Sol. Energy Mater. Sol. Cells **75**, 261 (2003).